

# Revival of a Canadian CPT Calibration Chamber

Wei Liu, Setare Setarenejad

*Department of Civil and Mineral Engineering – University of Toronto, Toronto, Ontario, Canada*

Jamie Sharp

*ConeTec Group, Vancouver, British-Columbia, Canada*

Mark Talesnick

*Department of Civil Engineering and Environmental Engineering – Technion Israel Institute of Technology, Haifa, Israel*

Mason Ghafghazi

*Department of Civil and Mineral Engineering – University of Toronto, Toronto, Ontario, Canada*



## ABSTRACT

Calibration chamber tests have been used worldwide to develop general or soil-specific CPT interpretation correlations for over half a century. Some of the most fundamental contributions to CPT interpretation and soil mechanics came from Golder Associates' calibration chamber in Calgary through the work of the late Ken Been and coworkers. In the 80s and 90s, important testing programs were supported by oil exploration in the Beaufort Sea and oil sands before the chamber was repurposed and eventually decommissioned in the 2000s. The chamber was donated to the University of Toronto in 2018. This paper summarizes the process of recommissioning that chamber and describes a test performed and innovative measurements made. A series of sensors were used to measure the strains and stresses that soil experiences as the cone advances. The sample preparation process, boundary conditions, cone push system, and post-test measurements are discussed.

## RÉSUMÉ

Les essais chambre calibrée ont été utilisés dans le monde pour développer les corrélations d'interprétations CPT générales et spécifiques au sol depuis plus d'un demi-siècle. Certaines des contributions les plus fondamentales à l'interprétation du CPT et à la mécanique des sols proviennent de la chambre calibrée de Golder Associates à Calgary par le travail de le feu Ken Been et ses collègues. Dans les années quatre-vingt et les années quatre-vingt-dix, programmes d'essais importants ont été soutenus par l'exploration pétrolière dans la mer de Beaufort et plus tard par les sables pétroliers avant la chambre qu'elle ne soit repurposé et déclassée dans les années 2000. La chambre a été donnée à l'Université de Toronto en 2018. Cet article résume la procédure de remise en service de la chambre et une brève description des essais effectués et des mesures innovantes effectuées. Une série des capteurs a été utilisée pour mesurer localement les contraintes et les déformations par le sol à mesure que le cône avance. La procédure de préparation de l'échantillon, les conditions limites, système de poussée du cône, et mesures après les essais sont discutés.

## 1 INTRODUCTION

The Cone Penetration Test (CPT) is rapidly becoming the primary geotechnical site investigation tool for various applications, including liquefaction assessment (Robertson and Campanella, 1985; Robertson and Wride, 1998; Shuttle and Cunniff, 2007; Ku and Juang, 2012). In practice, liquefaction analysis on sand either explicitly or implicitly starts by determining its in-situ state parameter and then judging whether it is susceptible to liquefaction, followed by the further evaluation of liquefaction resistance, triggering, and potential consequences. Been et al. (1985) proposed the state parameter to represent the in-situ density of sand based on critical state soil mechanics. Most existing CPT interpretation correlations were developed from calibration chamber tests (Been and Jefferies, 1987b; Houlsby and Hitchman, 1988; Schniadt and Houlsby, 1992; Wesley, 2002).

Calibration chambers are large circular steel tanks, typically 1 m in diameter and similar height. Approximately two tons of sand is deposited into a chamber at a known

density and consolidated to the desired stress, and then a CPT test is conducted in the same way as in the field. A series of calibration chamber tests on different samples with various densities and confining stresses can provide a soil-specific correlation between CPT measurements, stress conditions, and density.

There have been approximately 30 active chambers in the world since the 1980s with different dimensions, boundary conditions, deposition procedures, and capability to handle saturated specimens (Liu, 2018). However, some of the most fundamental contributions to CPT interpretation, especially on state parameter interpretation, came from Golder Associates' (now WSP Golder) calibration chamber in Calgary through Ken Been and his coworkers (Been and Jefferies, 1986; Been et al., 1987a; Been et al., 1987b). In the 80s and 90s, important testing programs were supported by oil exploration in the Beaufort Sea (Been et al., 1987b) and oil sands (Golder Associate, 1987) before the chamber was repurposed and eventually decommissioned in the 2000s. The chamber was donated to the University of Toronto in 2018. This

paper summarizes the process of recommissioning that chamber and a brief description of the tests performed and innovative measurements made. The sample preparation, boundary conditions, cone pushing system, and post-test measurements are discussed.

## 2 APPARATUS

### 2.1 Calibration Chamber

Been's calibration chamber testing system (Been et al., 1987b) was recommissioned at the University of Toronto. It was positioned in a pit to give better access and overhead space. A 2-ton crane was installed above it for moving parts and materials. A specially designed osmosis system can de-air tap water in real-time for saturating samples. Fig 1 depicts the calibration chamber with components labeled, and Fig 2 shows the schematic diagram of the chamber.

This chamber can accommodate a soil sample up to 1.14 m deep and 1.4 m in diameter. Stresses up to 700 kPa can be applied. If required, back pressure can also be applied for the saturation process. A manually controlled system fed by a pressurized air supply is used to impose a variety of stress conditions on the sample using three air-water reservoirs (one reservoir each for  $\sigma_v$ ,  $\sigma_h$  and back pressure). The chamber sits on three load cells with a capacity of 2 tons each. The load cells are used to keep track of the change in weight during the test, which is used to determine the sample void ratio at each stage (sample preparation and consolidation). The hydraulic jack sits on a reaction frame connected to the chamber's base, so the reaction force induced by cone penetration would not change the load cell readings and put additional demand on the surrounding structures and foundation.

The CPT probe used was provided by ConeTec, and it is a standard cone with a 10 cm<sup>2</sup> projected tip area (i.e., 3.57 cm in diameter) and 150 cm<sup>2</sup> friction sleeve area. The probe has three main channels to measure tip resistance ( $q_c$ ), sleeve friction ( $f_s$ ), and pore water pressure. The pore pressure is measured behind the shoulder of the cone ( $u_2$  position, ASTM D5778-12).

The cone can be advanced into the sample at variable rates from 0.02 to 2 cm/sec by a servo-controlled hydraulic jack with a maximum force of 50 kN. Pushing the cone slower than the standard rate (2 cm/sec) helps conduct tests on intermediate soils or silt-rich tailings.

### 2.2 Chamber size and boundary effects

Calibration chamber data requires a correction factor due to size and boundary effects because the calibration chamber wall is not as infinite as in the field, and no practical chamber can represent an actual field condition (Parkin et al., 1982; Mayne and Kulhawy, 1991; and Salgado et al., 1998).

The chamber has a chamber to standard cone-diameter ratio of 38. A ratio greater than 50 is desirable to minimize size effects for dense sand; however, for medium or loose sands, a 1.4 m diameter is adequate, and modest adjustments are required for chamber size and boundary effects (Been et al., 1987b).

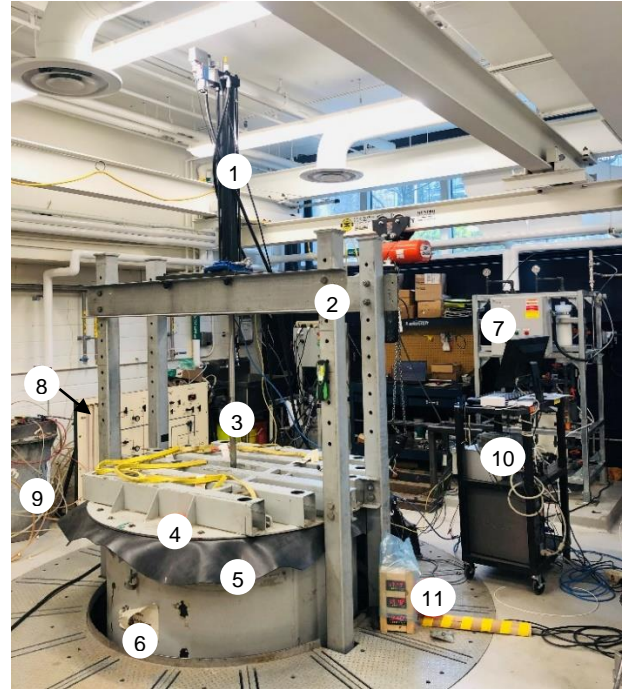


Figure 1. Calibration chamber testing system at UofT  
1-Hydraulic push system; 2-Reaction frame; 3-Cone rod; 4-Chamber lid; 5-Membrane; 6-Chamber wall; 7-De-airing system; 8-Pressure panel; 9-Air-water reservoir; 10-Data collecting unit; 11-Load cells readout

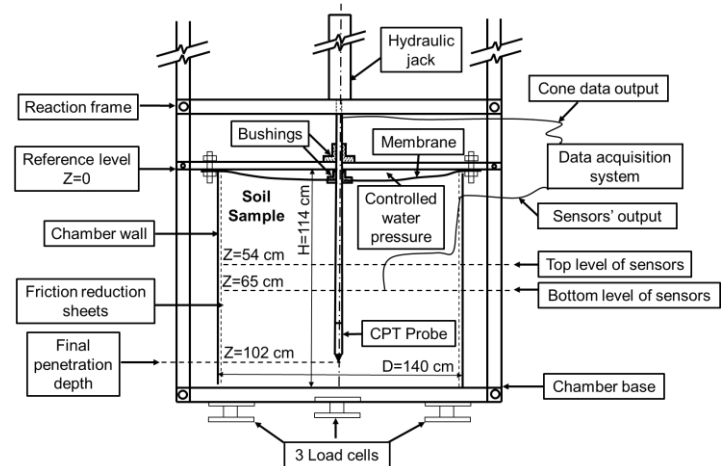


Figure 2. Schematic of the chamber showing one example with sensors levels indicated

The chamber can accommodate two boundary conditions. A schematic of the original boundary condition of the chamber is shown in Fig 3 (a), where constant vertical and horizontal stresses are applied independently to the soil specimen. More details about the modification of the chamber and testing procedures can be found in (Liu et al., 2019). A new  $k_0$  boundary condition (zero lateral strain), as shown in Fig 3 (b), was utilized as an alternative. In this setup, only one seal needs to be ensured in the top chamber cavity, where the vertical stress is applied to the soil sample through a membrane. The zero lateral strain condition is automatically constrained due to the relatively

rigid lateral wall of the chamber. It provides a more robust alternative with the potential to reduce boundary effects (Been et al.,1987a). No information was compromised, given that horizontal stresses are measured as described later.

Tests were performed under both boundary conditions using the same sand reconstituted by the same method. Results have shown a reasonable agreement once the tip resistance was normalized for the influence of confining stresses.

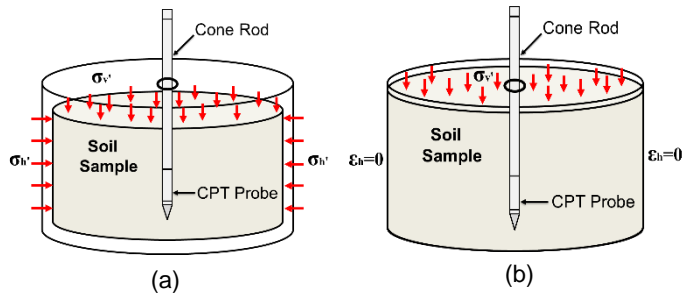


Figure 3 (a) Constant stresses boundary condition; (b)  $k_0$  wall boundary condition.

### 2.3 Stress and Strain Sensors

Understanding soil's stress and strain response developed during CPT penetration is essential to improve the interpretation and validate numerical models. High-quality calibration chamber tests on the sand with reliable local stress and strain measurements provide new insights into how soil and cone interact during penetration and how this interaction contributes to CPT measurements.

Three Null pressure sensors designed to measure normal pressures in soil were used in the chamber. The Null pressure sensor was initially designed by Talesnick (2005). The results from his research have illustrated that the sensor can accurately measure stresses in soil with less than 5% error (Talesnick, 2013). Compared to other normal pressure cells, the crucial design feature of this sensor is that it measures stresses without deforming. It can avoid arching effects that adversely influence soil stress measurements, especially during unloading. Results have shown that the measurement accuracy from this sensor is independent of the soil type, density, and stress history (Talesnick, 2013).

Three mini LVDTs (Linear Variable Displacement Transducer) designed to measure normal strains with a soil mass were used in the chamber. Talesnick's research group also developed these sensors, and more details can be found in Omer (2018).

Newly designed shear strain and stress sensors were also deployed in the chamber. Together, these measurements produced the complete state of strain and stress at a given point in the soil during cone penetration.

## 3 MATERIAL AND TESTING PROCEDURES

### 3.1 Material Tested

The sand tested in this chamber was obtained from Hutcheson quarry located in Huntsville, Ontario, referred to as Medium Hutcheson Sand (MHS) throughout the paper. The grain size distribution of MHS is shown in Fig 4, and material properties are given in Table 1.

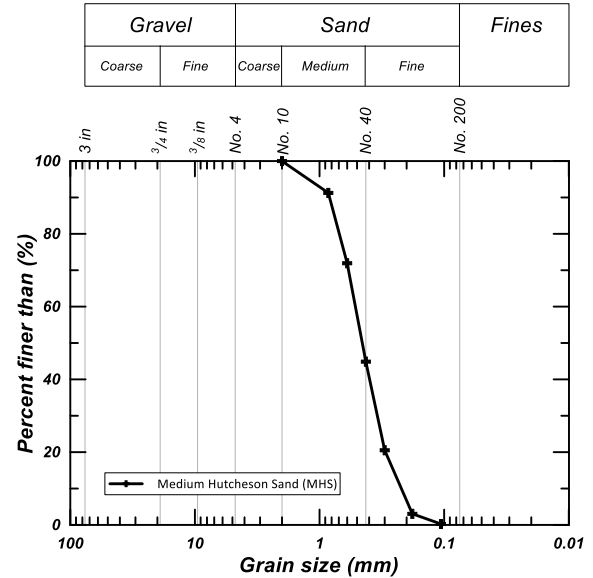


Figure 4. Gradation of Medium Hutcheson Sand

Table 1. Index properties of MHS

Material Characteristics	
$G_s$	2.7
$e_{max}$	0.877
$e_{min}$	0.602
Critical state parameters:	
$M_{tc}$	1.28
$\phi_{cs} (^{\circ})$	32
$\lambda_{10}$	0.089
$\Gamma$	0.97
Mean grain size, $D_{50}(mm)$	0.42
Effective grain size, $D_{10}(mm)$	0.22
Uniformity coefficient $D_{50}/D_{10}$	1.9
Percent passing:	0
No.200 sieve (fines content)	
Particle shape	Sub rounded to well rounded
Minerology	31% quartz, 45% feldspar, 15 % amphibole, 6% biotite, and 2% other



### 3.2 Sample Preparation

Before starting the sample preparation, it is essential to place two layers of friction reduction sheets on the inner wall of the chamber, as shown in Fig 5. The friction reduction sheets are made of polyethylene and lubricated with graphite lube in between two layers to reduce the friction between the soil and the inner wall of the chamber. This process helps the vertical pressure to be uniformly transferred from the top membrane throughout the soil specimen.

In calibration chamber tests, the air pluviation method is widely used because it can reconstitute a large sample quickly. The apparatuses used to achieve the pluviial deposition can be divided into stationary pluviators and traveling pluviators. Generally, the traveling pluviator performs better than the stationary pluviator as it can reduce the spatial variability of the specimen density and gradation. More details about the methods' principal, strengths, and drawbacks can be found in Fretti (1995).

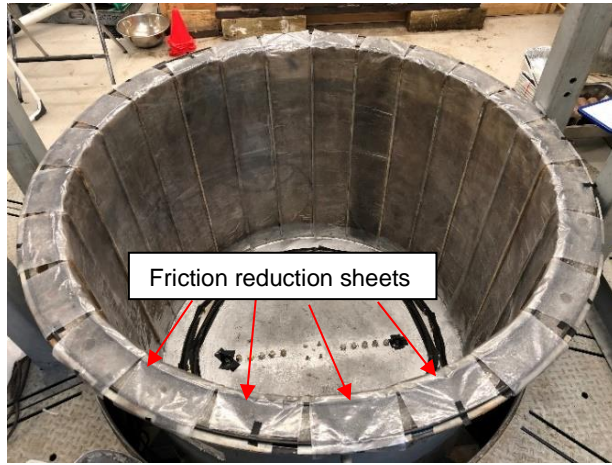


Figure 5. Friction reduction sheets on the inner wall of the chamber

A traveling pluviator was adopted, and the schematic of the setup is shown in Fig 6. A rigid PVC pipe with sieves attached below is connected to a flexible funnel made of fabric and then attached to a steel hopper lifted by the crane. The hopper is manually moved back and forth over the specimen surface at a constant speed, following the paths illustrated on the right in Fig 6. The drop height is held constant by controlling the crane up and down with a rod as a reference.

A rigid pipe 10 cm in diameter and two sieves with 2 mm openings immediately below the rigid pipe were used to control the deposition intensity (i.e., the amount of soil falling per unit of area and per unit of time). The average void ratio of the reconstituted sample was  $e_0 = 0.622$  ( $Dr = 92\%$ ) for a drop height of 40 cm. Loose samples can also be obtained by increasing the opening of sieves and decreasing the drop height. Generally, drop heights between 5 and 40 cm, with or without sieves, produced relative densities between 20 and 90%.

The entire sample preparation process takes about 15 hours by two people, and the dust raised during the sand deposition can be easily removed by a dust collector. Fig 7 shows the entire soil sample after preparation is

completed. The cone measurements and post-test sampling will confirm the uniformity of the sample.

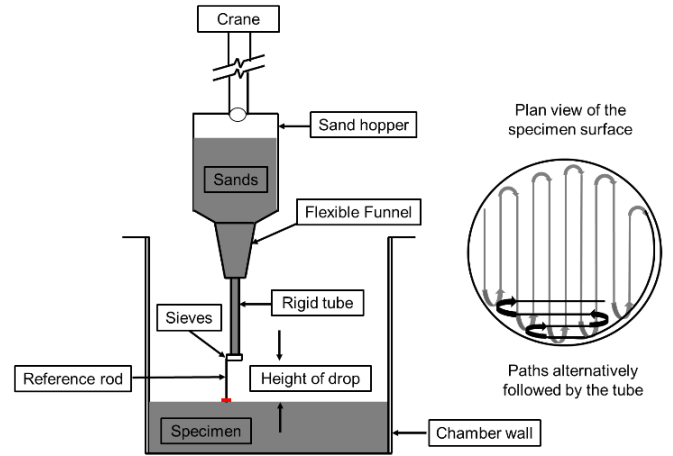


Figure 6. Scheme of traveling pluviator for the sample preparation



Figure 7. Picture of an entire soil sample with surface flatted

### 3.3 Sensor Placement

Sand pluviation was halted twice to allow sensors to be placed at two levels with depths indicated in Fig 2. The sensors are radially placed at the same distance from the center of the cone ( $R = 3d_{cone} = 10.7 \text{ cm}$ ). The distance was determined from the geometric center of the sensor to the center of the cone. Fig 8 shows the layout of the sensors on two levels, where all stress components ( $\sigma_z, \sigma_r, \sigma_\theta, \tau_{rz}$ ) and strain components ( $\varepsilon_z, \varepsilon_r, \varepsilon_\theta, \gamma_{rz}$ ) at one point ( $R = 3d_{cone}$ ) were measured as the cone advances.

The sensor data are shifted in post-processing to account for the different depths. The point when the tip of the cone arrives at each level of sensors is taken as the reference depth.

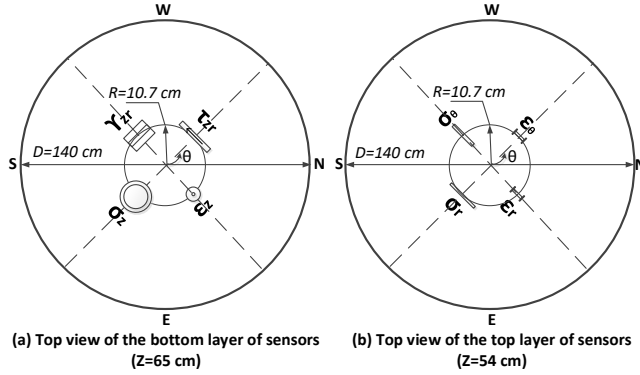


Figure 8. Sensors' layout on two levels in the chamber

### 3.4 CPT test

After sample preparation and placement of sensors, the chamber closed, followed by mounting of the reaction frame and hydraulic jack. The soil sample was then consolidated to  $\sigma_v = 100 \text{ kPa}$  under  $K_0$  conditions with volume change recorded. The cone was then pushed slower (0.5 cm/sec) than the standard rate (2 cm/sec). Penetration rate has no effect in dry sand, so this slower rate was adopted for better control and higher resolution in measurements.

### 3.5 Post-Test Procedures

After the test, the cone was retracted, the sample was unloaded, and careful sampling was done to measure void ratios and particle breakage levels locally. Although the sample uniformity was confirmed by the constant measurements of  $q_c$  and  $f_s$  in the middle of the penetration range, it is still helpful to check the uniformity by sampling. The sample was manually removed layer by layer. For measuring void ratios, three thin-walled tubes (0.3 mm thick, 10 cm in diameter, and 10 cm long) were used to obtain three samples at 15, 30, and 50 cm radii away from the center of the chamber after every 15 cm of removal. A thin-wall tube sampler (6.5 cm in diameter and 10 cm long) was used to sample sand from the chamber's center at every 15 cm depth for sieving. The tubes were pushed in, and the surrounding sand was removed before a thin plate was inserted underneath.

## 4 RESULTS

### 4.1 CPT and Sampling data

Fig 9 (a) shows tip resistance and sleeve friction trace during the penetration on a dense sample ( $e = 0.595$  and  $\psi = -0.22$ ) consolidated to 100 kPa vertical stress. The horizontal stress required to calculate the mean effective stress for calculating the state parameter was measured from two Null pressure sensors. The  $q_c$  and  $f_s$  values reached a constant level (13.5~14 MPa, 40~50 kPa) over the 45-75 cm penetration range, and they increased at greater depths from 75 cm (equal to the distance of 10 times the cone's diameter above the rigid base,  $h/d = 10$ ) as expected from boundary effects at the

bottom. A slight increase (3~5%) in  $q_c$  was also observed when the cone reached the two levels of sensors.

A detailed sample void ratio profile was obtained from the measurements on the post-test samples, as shown in Fig 9 (b). The average void ratio from the tube samples was generally close to the void ratio after the consolidation obtained based on the known total sample dimensions, measured weight, and volume change. In general, the variability of void ratio for this test is less than 0.05, suggesting a high-quality uniform specimen (Been et al., 1987b).

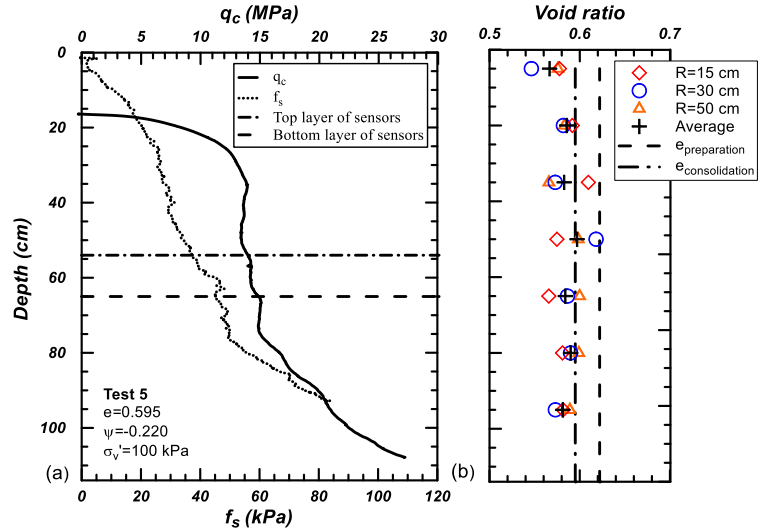


Figure 9. (a) Profiles of cone data, (b) sampling results along with the depth.

### 4.2 Particle breakage

Particle breakage typically occurs near the tip of the cone due to the significant increase in the mean stress and shear stresses during penetration. Figure 10 (a) presents grain size distribution curves for the samples collected at various depths after the test. The sample collected at  $Z=5 \text{ cm}$  depth showed no crushing because the initial position of the cone before pushing was below this level. Deeper samples showed a change in particle size distributions marked by up to a 4.5% increase in the fines content due to the particle breakage. Fig 10 (b) presents the change in fines content (percentage passing for the No. 200 sieve (0.075mm opening) at different sample depths. Slightly more fines were found as the cone advanced deeper, which may be attributed to the higher tip resistance mobilized due to the rigid boundary near the bottom or cave-in of surrounding materials after the cone was retrieved.

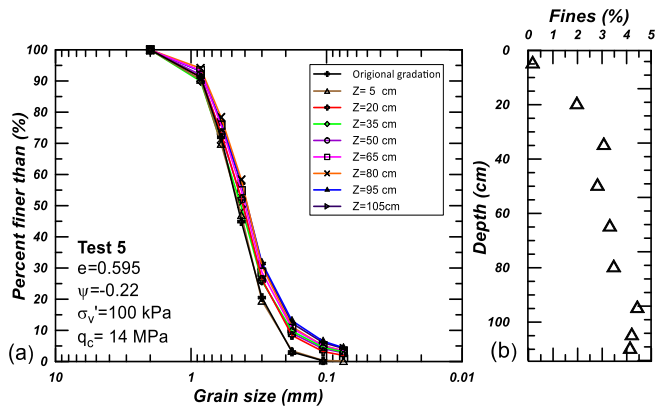


Figure 10 (a): Particle size distribution curves before and after test at different sample depths; (b) percentage of fines passing No. 200 sieve caused by particle breakage.

## 5. SUMMARY

This paper summarized the process of modifying and recommissioning the chamber donated by WSP Golder to the University of Toronto and described testing procedures and example data from one test performed on dry sand in a dense state. A series of sensors were used to locally measure the strains and stresses that soil experiences as the cone advances. The sample preparation, boundary conditions, CPT results, and post-test measurements were discussed.

## 6. ACKNOWLEDGEMENTS

The authors greatly appreciate the financial support of Klohn Crippen Berger, ConeTec, WSP Golder, NSERC, and the Chinese Scholarship Council (CSC). The authors also extend their special thanks to Dr. Dennis Becker for donating the chamber to University of Toronto.

## 7. REFERENCES

American Society for Testing and Materials D5778-12 (2012). "Standard test method for electronic friction cone and piezocone penetration testing of soils." Annual Book of ASTM Standards, 4, 1587-1605.

Been, K., Crooks, J. H. A., Becker, D. E., & Jefferies, M. G. (1986). The cone penetration test in sands: part I, state parameter interpretation. *Géotechnique*, 36(2), 239-249.

Been, K., Jefferies, M. G., Crooks, J. H. A., & Rothenburg, L. (1987a). The cone penetration test in sands: part II, general inference of state. *Géotechnique*, 37(3), 285-299.

Been, K., Lingnau, B. E., Crooks, J. H. A., & Leach, B. (1987b). Cone penetration test calibration for Erksak (Beaufort Sea) sand. *Canadian Geotechnical Journal*, 24(4), 601-610.

Fretti, C., Presti, D. L., & Pedroni, S. (1995). A pluvial deposition method to reconstitute well-graded sand specimens. *Geotechnical Testing Journal*, 18(2), 292-298.

Golder Associates (1987) Cone penetration tests on Syncrude Tailings, Technical report, No. 872-2402.

Houlsby, G. T., & Hitchman, R. (1988). Calibration chamber tests of a cone penetrometer in sand. *Géotechnique*, 38(1), 39-44.

Ku, C. S., & Juang, C. H. (2012). Liquefaction and cyclic softening potential of soils a unified piezocone penetration testing-based approach. *Géotechnique*, 62(5), 457-461.

Liu, W. (2018) Interpretation of cone penetration test in silty sand and tailings through calibration chamber testing. (Ph.D. Research Proposal, Department of Civil and Mineral Engineering, University of Toronto.

Liu, W., Azubalis, A., & Ghafghazi, M. (2019). Commissioning of a Large Calibration Chamber for Cone Penetration Test in Silty Sands and tailings. *In Proc., 6<sup>th</sup> International Conference on Geotechnical and Geophysical Site Characterisation, Budapest, Hungary.*

Lunne, T., Powell, J. J., & Robertson, P. K. (2002). Cone penetration testing in geotechnical practice. CRC Press.

Mayne, P. (1991). Calibration chamber database and boundary effects correction for CPT data. *In Proc. 1st Int Symp. on Calibration Chamber Testing* (pp. 257-264).

Omer, I. (2018) Development of a Methodology for the Use of a Push-in Pressure Cell in Sand, through Investigation of the Penetration Mechanism of a Pile, Master Thesis, Technion-Israel Institute of Technology.

Parkin, A. K., & Lunne, T. (1982). Boundary effects in the laboratory calibration of a cone penetrometer for sand. *Norwegian Geotechnical institute publication*, (138).

Robertson, P. K., & Campanella, R. G. (1985). Liquefaction potential of sands using the CPT. *Journal of Geotechnical Engineering*, 111(3), 384-403.

Robertson, P. K., & Wride, C. E. (1998). Evaluating cyclic liquefaction potential using the cone penetration test. *Canadian Geotechnical Journal*, 35(3), 442-459.

Salgado, R., Mitchell, J. K., & Jamiolkowski, M. (1998). Calibration chamber size effects on penetration resistance in sand. *Journal of Geotechnical and Geoenvironmental Engineering*, 124(9), 878-888.

Schnaid, F., & Houlsby, G. T. (1992). Measurement of the properties of sand in a calibration chamber by the cone penetrometer test. *Géotechnique*, 42(4), 587-601.

Shuttle, D. A., & Cunning, J. (2007). Liquefaction potential of silts from CPTu. *Canadian Geotechnical Journal*, 44(1), 1-19.

Talesnick, M. (2005). Measuring soil contact pressure on a solid boundary and quantifying soil arching. *Geotechnical Testing Journal*, 28(2), 171-179.

Talesnick, M. (2013). Measuring soil pressure within a soil mass. *Canadian Geotechnical Journal*, 50(7), 716-722.

Wesley, L. D. (2002). Interpretation of calibration chamber tests involving cone penetrometers in sands. *Géotechnique*, 52(4), 289-293.